

Model Predictive Robustness of Signal Temporal Logic Predicates

Yuanfei Lin^{*,1}, Haoxuan Li^{*,2}, and Matthias Althoff¹

Abstract—The robustness of signal temporal logic not only assesses whether a signal adheres to a specification but also provides a measure of how much a formula is fulfilled or violated. The calculation of robustness is based on evaluating the robustness of underlying predicates. However, the robustness of predicates is usually defined in a model-free way, i.e., without including the system dynamics. Moreover, it is often nontrivial to define the robustness of complicated predicates precisely. To address these issues, we propose a notion of model predictive robustness, which provides a more systematic way of evaluating robustness compared to previous approaches by considering model-based predictions. In particular, we use Gaussian process regression to learn the robustness based on precomputed predictions so that robustness values can be efficiently computed online. We evaluate our approach for the use case of autonomous driving with predicates used in formalized traffic rules on a recorded dataset, which highlights the advantage of our approach compared to traditional approaches in terms of expressiveness. By incorporating our robustness definitions into a trajectory planner, autonomous vehicles obey traffic rules more robustly than human drivers in the dataset.

I. INTRODUCTION

Formal methods are crucial for specifying and verifying the behaviors of autonomous robotic systems [1]. Temporal logic, such as linear temporal logic (LTL) [2], metric temporal logic (MTL) [3], and signal temporal logic (STL) [4], allows one to specify safety properties and unambiguous tasks for a system over time. A prominent example is the traffic rules for autonomous vehicles on which we focus in this paper. MTL and STL are additionally equipped with quantitative semantics, i.e., robustness (aka robustness degree) [5], [6], returning the degree of satisfaction or violation of a system with respect to a given specification. In this work, we focus on specifications formalized in STL since one can easily represent discrete-time MTL formulas in STL [7] and recent research on improving the robustness mainly addresses STL.

The robustness of predicates is an essential building block for evaluating the robustness of STL formulas. However, the robustness of STL predicates is typically defined in a model-free way, i.e., without considering the underlying system dynamics. Therefore, the model-free robustness does not embody or predict the real capability of the system to meet the predicates, which is addressed in this work (see the general idea in Fig. 1).

* The first two authors have contributed equally to this work.

¹Yuanfei Lin and Matthias Althoff are with the School of Computation, Information and Technology, Technical University of Munich, 85748 Garching, Germany.

²Haoxuan Li is with the School of Engineering and Design, Technical University of Munich, 85748 Garching, Germany.

{yuanfei.lin, haoxuan.li, althoff}@tum.de

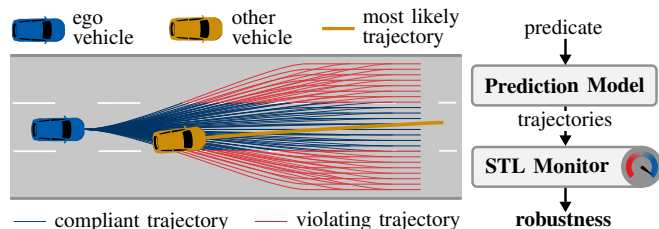


Fig. 1: Scheme of model predictive robustness computation for the predicate `in_same_lane`. The prediction model generates a finite set of trajectories for all rule-relevant vehicles within a certain time period, of which the rule compliance is checked by the STL monitor. The robustness is calculated based on the future probability of satisfying the predicate.

A. Related Work

Our robustness definition aims to facilitate online planning and control with temporal logic specifications. Subsequently, we present related works on specification formalization, model-free robustness, and nonlinear regression approaches for online applications.

a) *Specification Formalization*: The development of autonomous vehicles requires planning and control to fulfill formal specifications. Several publications formalize traffic rules for interstates [3], [8], intersections [9], and marines [10] in MTL. They use parameterizable Boolean predicates and functions in higher-order logic to specify basic elements of rule specifications. In [4], [11], [12], safety requirements are specified in STL together with the robustness definition for formal verification and controller synthesis.

b) *Model-free Robustness*: The robustness of STL is typically nonconvex and nondifferentiable, e.g., in [6]. Therefore, it is generally difficult to deploy fast gradient-based optimization algorithms for online usage, such as optimization-based trajectory planning for autonomous vehicles [13]. Many new extensions for STL robustness have been proposed to address this issue. In [14]–[17], smooth approximations are applied to make the robustness differentiable. To handle complex specifications efficiently, [18] considers STL formulas over convex predicates. However, these works only refine the robustness calculation for temporal and logical operators while using affine functions as the robustness of predicates.

For uncertain and changing environments, a probabilistic variant of STL is proposed to express safety constraints on random variables and stochastic signals in [19]–[21]. Similarly, Lee *et al.* [22] extend STL with uncertain events as predicates to formulate a controller synthesis problem as probabilistic inference. Nevertheless, these works only evaluate the signal in the form of probability distributions instead of the robustness based on stochastic methods. For instance, the risk of violating safety specifications is estimated by

a random variable in [23], where the gap between system dynamic models and the probability calculation is, however, not yet bridged since the latter only evaluates states.

c) *Nonlinear Regression*: Supervised learning algorithms, e.g., regression and classification, have been used to model relationships between variables to improve prediction accuracy and computational efficiency. For safety-critical applications, Gaussian processes (GPs) [24] have drawn more and more attention since they are flexible and nonparametric¹. In addition, GP regression can provide uncertainties for its prediction, which is used to improve the safety and robustness of model predictive control in [25]–[27]. In this regard, we are inspired by the regression approach described in [28], where a GP model is used for estimating the robustness of STL specifications including levels of uncertainty. But a more general observation space is adapted for regression in this paper.

B. Contributions

We present a novel approach to determine the robustness of STL predicates, where the model capability of rule compliance is explicitly considered. When defining a new predicate, the robustness can be directly computed based on its Boolean evaluation instead of relying on manually tuned heuristics. In particular, our contributions are:

- 1) proposing for the first time a systematic robustness metric for STL predicates based on predictive models;
- 2) using GP regression to learn robustness with comprehensive input features for online applications; and
- 3) demonstrating the effectiveness of our robustness definition on formalized traffic rules with real-world data.

The remainder of this paper is organized as follows: In Sec. II, required preliminaries and formulations are introduced. Sec. III provides an overview of the model predictive robustness definition and computation. In Sections IV, GP regression is presented to learn the robustness of predicates. We demonstrate the benefits of our method by numerical experiments in Sec. V, followed by conclusions in Sec. VI.

II. PRELIMINARIES

A. System Description and Notation

We model the dynamics of vehicles as discrete-time systems:

$$x_{k+1} = f(x_k, u_k), \quad (1)$$

where $x_k \in \mathbb{R}^{n_x}$ is the state, $u_k \in \mathbb{R}^{n_u}$ is the input, and the index $k \in \mathbb{N}_0$ is the discrete time step corresponding to the continuous time $t_k = k\Delta t$ with a fixed time increment $\Delta t \in \mathbb{R}^+$. We use a curvilinear coordinate system [29] that is aligned with a reference path Γ (e.g., the lane centerline), as shown in Fig. 2. The position of the vehicle at time step k is described by the arc length s_k along Γ and the orthogonal deviation d_k to Γ at s_k . The states and the inputs are bounded by sets of permissible values: $\forall k : x_k \in \mathcal{X}_k, u_k \in \mathcal{U}_k$. We denote a possible solution of (1) at time step $\tau \geq k$ by

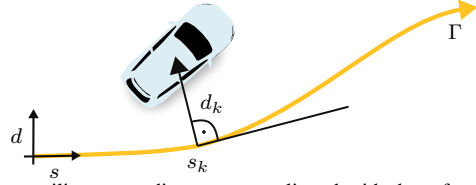


Fig. 2: A curvilinear coordinate system aligned with the reference path Γ .

the state trajectory $\chi(\tau, x_k, u([k, \tau]))$ for an initial state x_k and an input trajectory $u([k, \tau])$. The set of possible state trajectories for the time interval $[k, \tau]$ is denoted as $\mathcal{X}_{[k, \tau]}$.

We introduce the following sets: $\mathcal{B} \subset \mathbb{N}$ is the set of indices referring to rule-relevant obstacles, $\mathcal{L} \subset \mathbb{N}$ contains the indices of the occupied lanes by a vehicle, and $\mathcal{L}^c \subseteq \mathcal{L}$ is the subset of \mathcal{L} comprising the occupied lane by the vehicle center. The road boundary is denoted as \flat . Let \square be a variable, we denote its value associated with the ego vehicle, i.e., the vehicle to be controlled, by \square_{ego} and with other obstacles by \square_b , with $b \in \mathcal{B}$. For regression models, we use feature variables containing the relevant vehicular and environmental information as the inputs $\mathbf{z} \in \mathbb{R}^{n_z}$ and the corresponding robustness as the output $y \in \mathbb{R}$. The feature variables $\mathbf{z} = \mathbf{o}(\omega_k)$ are obtained via an observation function $\mathbf{o} : \mathcal{X}_k^{|\mathcal{B}|+1} \rightarrow \mathbb{R}^{n_z}$, where the vector $\omega_k = (x_{\text{ego}, k}, x_{1, k}, \dots, x_{|\mathcal{B}|, k})^T \in \mathcal{X}_k^{|\mathcal{B}|+1}$ consists of the state vectors of the ego vehicle and other rule-relevant obstacles at time step k .

B. Signal Temporal Logic

For traffic rule monitoring, we consider a discrete-time signal $\omega := \omega_0 \dots \omega_k \dots \omega_{n_\omega}$ representing a sequence of vectors ω_k . Given formulas φ , φ_1 , and φ_2 , the STL syntax is defined as [7, Sec. 2.1]:

$$\varphi := p \mid \neg\varphi_1 \vee \varphi_2 \mid \varphi_1 \mathbf{U}_I \varphi_2, \quad (2)$$

where $p := \alpha(\omega_k) \sim 0, \sim \in \{>, \geq\}$, is an atomic predicate defined by the evaluation function $\alpha : \mathcal{X}_k^{|\mathcal{B}|+1} \rightarrow \mathbb{R}$, \neg and \vee are the Boolean *negation* and *disjunction* operators, respectively, and \mathbf{U}_I is the *until* operator requiring φ_1 to remain true until φ_2 becomes true in a time interval $I \subseteq \mathbb{N}_0$. As a result, the predicate p is either true (\top) or false (\perp). Other logical connectives and temporal operators can be constructed from (2) such as the *future* (aka *eventually*) operator $\mathbf{F}_I \varphi := \top \mathbf{U}_I \varphi$ [7, Sec. 2.1].

To show whether an STL formula is satisfied with qualitative semantics, we introduce the characteristic function:

Definition 1 (Characteristic Function [6, Def. 1]):

The characteristic function $c : \mathcal{X}_k^{|\mathcal{B}|+1} \rightarrow \{-1, 1\}$ of an STL formula φ related to a signal ω at time step k is defined as:

$$\begin{aligned} c(p, \omega, k) &:= \begin{cases} 1 & \text{if } p = \top \\ -1 & \text{if } p = \perp \end{cases} \\ c(\neg\varphi, \omega, k) &:= -c(\varphi, \omega, k) \\ c(\varphi_1 \vee \varphi_2, \omega, k) &:= \max(c(\varphi_1, \omega, k), c(\varphi_2, \omega, k)) \\ c(\varphi_1 \mathbf{U}_I \varphi_2, \omega, k) &:= \max_{\tau \in (k+I) \cap \mathbb{N}_0} \left(\min(c(\varphi_2, \omega, \tau), \right. \\ &\quad \left. \min_{\tau' \in (k, \tau)} (c(\varphi_1, \omega, \tau')) \right). \end{aligned} \quad (3)$$

¹We refer to the nonparametric model as a model with unfixed numbers of parameters with respect to the size of the used data.

The model-free STL quantitative metric is presented as:

Definition 2 (Model-free Robustness [6, Def. 3]):

The model-free robustness ρ^{MF} of a predicate p with respect to a signal ω at time step k is defined using the evaluation function α as:

$$\rho^{\text{MF}}(p, \omega, k) := \alpha(\omega_k). \quad (4)$$

The calculation of other operators uses the same mathematical principles as presented in Def. 1.

C. Problem Formulation

Inspired by the metrics described in [15], [23], the robustness of STL predicates should follow the subsequent properties to facilitate its application to planning and control problems:

Property 1 (Soundness):

Positive robustness is a necessary and sufficient condition for satisfying the predicate; likewise, a signal has negative robustness for violating the predicate.

Property 2 (Smoothness):

The robustness is smooth with respect to its input elements almost everywhere² except on the satisfaction or violation boundaries where $\alpha(\omega_k) = 0$.

Property 3 (Monotonicity):

The robustness increases with a growing probability of satisfying the predicate and decreases otherwise.

The soundness and smoothness can be considered by following the requirements in [15, Thm. 1 and Prop. 1]. For monotonicity, the robustness needs to rely on dynamic models and predictive behaviors of the described system, which we call the *model predictive robustness* since the idea is similar to what is used in model predictive control [30]. In this work, we mainly focus on traffic rule predicates, but our definition can be extended to other types of STL predicates.

III. MODEL PREDICTIVE ROBUSTNESS

In this section, the model predictive robustness is first formally defined. Then we introduce a Bayesian representation of the predictive model. Afterward, the overall algorithm for the computation of the robustness is presented, followed by its detailed description.

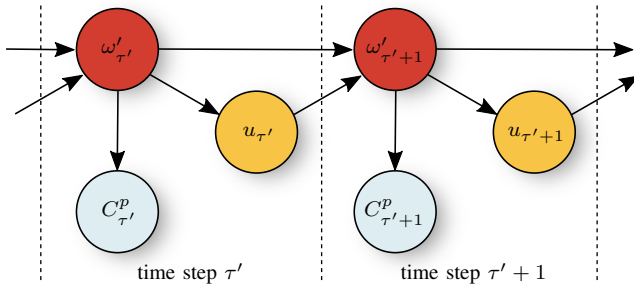


Fig. 3: Structure of the DBN for the prediction model of traffic rule compliance. Random variables and causal dependencies are illustrated as circles and solid arrows, respectively. The same type of random variables is marked with the same color.

²This is because smoothness across the entire domain is a too strict requirement for robustness metrics [17, Sec. IV].

A. Definition

Modeling the values of characteristic functions $c(p, \omega, \tau)$ of predicate p at time step $\tau \geq k$ as binary random variables C_τ^p , we define the model predictive robustness:

Definition 3 (Model Predictive Robustness):

The model predictive robustness ρ^{MP} considers the probability \bar{P} that the value of the characteristic function is unchanged over a finite prediction horizon $h \in \mathbb{N}_0$ and is defined as:

$$\rho^{\text{MP}}(p, \omega, k) := \begin{cases} \frac{\bar{P} - \bar{P}_{+, \min}}{\bar{P}_{+, \max} - \bar{P}_{+, \min}} & \text{if } c(p, \omega, k) = 1 \\ -\frac{\bar{P} - \bar{P}_{-, \min}}{\bar{P}_{-, \max} - \bar{P}_{-, \min}} & \text{if } c(p, \omega, k) = -1 \end{cases} \quad (5)$$

$$\text{s.t. } \bar{P} := \frac{1}{h+1} \sum_{\tau=k}^{k+h} P(C_\tau^p = c(p, \omega, k)),$$

where $\rho^{\text{MP}}(p, \omega, k)$ is normalized to the interval $[-1, 1]$ and the normalization constants $\bar{P}_{+, \max/\min} \in \mathbb{R}_0$ and $\bar{P}_{-, \max/\min} \in \mathbb{R}_0$ are obtained from the maximum/minimum values of P for positive and negative characteristic functions, respectively.

B. Bayesian Representation

To predict traffic rule satisfaction or violation, vehicle behaviors can be represented by probabilistic graphical models [31, Pt. I]. As an example, we describe the predicted behaviors as a dynamic Bayesian network (DBN) [31, Sec. 6.2.2] [32] since it can capture the spatio-temporal evolution of the prediction model in a compact form (cf. Fig. 3). The inputs are represented as hidden variables and the predicted signal is denoted as ω' . For simplicity, we assume the transition between states and the robustness evaluation to be deterministic. The probability of maintaining the value of the characteristic function at time step τ can be written as:

$$\begin{aligned} & P(C_\tau^p = c(p, \omega, k)) \\ &= \sum_{\omega'_\tau \in \Omega'_\tau} P(\omega'_\tau) P(C_\tau^p = c(p, \omega, k) | \omega'_\tau) \\ & \stackrel{\text{DBN [32, Sec. 2.2]}}{=} \sum_{\omega'_\tau \in \Omega'^c_\tau} \prod_{\tau'=k}^{\tau-1} \sum_{u_{\tau'} \in \mathcal{U}_k} P(u_{\tau'} | \omega'_{\tau'}), \end{aligned} \quad (6)$$

where Ω'_τ is the set of predictive signals ω'_τ , $\Omega'^c_\tau \subseteq \Omega'_\tau$ is its subset satisfying $C_\tau^p = c(p, \omega, k)$, and $P(C_\tau^p = c(p, \omega, k) | \omega'_\tau)$ is either 0 or 1 depending on ω'_τ due to the determinism. However, it is nontrivial to obtain the exact distribution of the transition probability $P(u_{\tau'} | \omega'_{\tau'})$ as shown in (6) [33, Sec. V]. Instead, we use sampling-based methods to obtain possible future behaviors of the ego vehicle. For other traffic participants, their most likely trajectories $\chi^{\text{ML}}_{[k, k+h]}$ are utilized as deterministic behaviors for simplicity of probabilistic inference. By assembling the sampled trajectories of the ego vehicle and the most likely trajectories of other vehicles, the Monte Carlo estimation of the probability in (5) at time step τ can be calculated as the ratio of the number of signal vectors in Ω'^c_τ to the size of Ω'_τ [34, Sec. 2.4]:

$$P(C_\tau^p = c(p, \omega, k)) \approx \frac{|\Omega'^c_\tau|}{|\Omega'_\tau|}. \quad (7)$$

C. Overall Algorithm

Alg. 1 provides an overview of the computation of the model predictive robustness for traffic rule predicates. At time step k , we receive as input the predicate, the current states of all rule-relevant vehicles, and the horizon h . First, we sample a set of trajectories $\mathcal{X}_{\text{ego},[k,k+h]}$ for the ego vehicle based on its current state (line 1; cf. Sec. III-D). Afterward, if the predicate is associated with other traffic participants, i.e., $|\mathcal{B}| > 0$, their most likely trajectories $\mathcal{X}_{\mathcal{B},[k,k+h]}^{\text{ML}}$ are determined (line 3; cf. Sec. III-E). Then the set of all predicted signals $\Omega' := \Omega'_k \dots \Omega'_\tau \dots \Omega'_{k+h}$ is constructed by the Cartesian product (line 7):

$$\begin{aligned} \mathcal{X}_{\text{ego},[k,k+h]} \times \mathcal{X}_{\mathcal{B},[k,k+h]}^{\text{ML}} &= \{\omega'_\tau | x_{\text{ego},\tau} \in \mathcal{X}_{\text{ego},[k,k+h]}, \\ &\forall b \in \mathcal{B}, x_{b,\tau} \in \mathcal{X}_{b,[k,k+h]}^{\text{ML}}, \tau \in [k, k+h]\}, \end{aligned} \quad (8)$$

which is followed by the computation of the robustness (line 8). Note that the normalization constants in (5) need to be precomputed, e.g., by evaluating the probability \bar{P} and characteristic functions on a dataset.

Algorithm 1 COMPUTEMODELPREDICTIVEROBUSTNESS

Input: predicate p , signal ω at time step k , horizon h

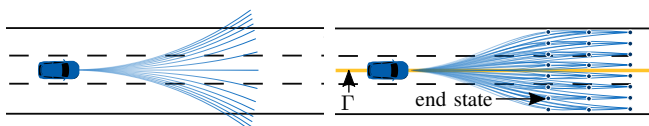
Output: model predictive robustness ρ^{MP}

- 1: $\mathcal{X}_{\text{ego},[k,k+h]} \leftarrow \text{SAMPLEEGOTRAJ}(\omega_k, h)$ \triangleright Sec. III-D
 - 2: **if** $|\mathcal{B}| > 0$ **then**
 - 3: $\mathcal{X}_{\mathcal{B},[k,k+h]}^{\text{ML}} \leftarrow \text{MOSTLIKELYTRAJ}(\omega_k, h)$ \triangleright Sec. III-E
 - 4: **else**
 - 5: $\mathcal{X}_{\mathcal{B},[k,k+h]}^{\text{ML}} \leftarrow \emptyset$
 - 6: **end if**
 - 7: $\Omega' \leftarrow \text{CARTESIANPRODUCT}(\mathcal{X}_{\text{ego},[k,k+h]}, \mathcal{X}_{\mathcal{B},[k,k+h]}^{\text{ML}})$ \triangleright (8)
 - 8: $\rho^{\text{MP}} \leftarrow \text{COMPUTEROBUSTNESS}(p, \Omega')$ \triangleright (5), (7)
 - 9: **return** ρ^{MP}
-

D. Trajectory Sampling for the Ego Vehicle

Trajectories can be sampled either in control space or in state space [35] (see Fig. 4). The former generates trajectories through the forward simulation of the vehicle dynamics. In contrast, with the state-based strategy, the trajectories are obtained by connecting pairs of vehicle states, which helps to exploit environmental constraints to avoid unnecessary samples. Since we only consider structured environments and want to provide more reactive capabilities for the ego vehicle, the state-space sampling approach described in [36] is used.

As shown in Fig. 4b, a set of end states at time step $k+h$ are distributed uniformly in the curvilinear coordinate system along the reference path Γ . Then trajectories are computed by connecting the end states with the current ego



(a) Sampling in control space.

(b) Sampling in state space.

Fig. 4: Comparison of different sampling strategies for the ego vehicle.

state at time step k using quintic polynomials. Afterward, the kinematic feasibility of the trajectories is checked, e.g., using the *CommonRoad Drivability Checker* [37], and the feasible ones are transformed from the curvilinear coordinate to the Cartesian frame as sampled trajectories.

E. Behavior Model of Other Vehicles

Various approaches for predicting the behaviors of surrounding vehicles are reviewed and compared in [38]. Simple kinematic models and pattern-based approaches are insufficient for our approach, since they might be unrealistic and no past observation before time step k is provided. Instead, we regard the trajectories for other vehicles from recorded data as their most likely behaviors, which is more suitable for learning purposes [39].

IV. GAUSSIAN PROCESS REGRESSION

Determining the model predictive robustness is computationally expensive and noisy due to discretization errors. As motivated in Sec. I-A, we choose the GP regression to learn the robustness.

A. Feature Variables

The discriminative capabilities of regression models highly depend on the selection of the feature variables [24, Sec. 7.5]. We define the observation of the feature variables \mathbf{z} in four categories as listed in Tab. I, which are either rule-related or commonly used for learning-based algorithms, e.g., in [39], [40]. To compute Δ_b or $\Delta_{\mathcal{L}^c}$, we use the signed distance from the vehicle center to its closest point at the boundary b or the bounds of lane \mathcal{L}^c .

TABLE I: Feature variable definition. All values presented are in SI units and at time step k unless otherwise specified.

Feature Variable	Description
Rule-Related	
$c(p, \omega, k)$	characteristic function
Ego-Vehicle-Related	
$l_{\text{ego}}, w_{\text{ego}}$	vehicle length and width
$x_{\text{ego}}, u_{\text{ego}}$	state and input
$\Delta_{\mathcal{L}_1^c, \text{ego}}, \Delta_{\mathcal{L}_r^c, \text{ego}}$	left and right distance to the left and right boundary of the occupied lane
$\Delta_{b_l, \text{ego}}, \Delta_{b_r, \text{ego}}$	distance to the left and right road boundary
Other-Vehicle-Related	
l_b, w_b	vehicle length and width
x_b	state
$\Delta_{\mathcal{L}_1^c, b}, \Delta_{\mathcal{L}_r^c, b}$	left and right distance to the left and right boundary of the occupied lane
$\Delta_{b_l, b}, \Delta_{b_r, b}$	distance to the left and right road boundary
Ego-Other-Relative	
Δ_s, Δ_d	relative longitudinal and lateral distance
Δv	relative velocity

B. Principles

A GP is a collection of random variables such that any finite subset of those variables is jointly Gaussian distributed [24, Def. 2.1]. With $n_p \in \mathbb{N}^+$ input-output pairs, the training set of GP is given by $\mathcal{D} = \{(\mathbf{z}_i, y_i)\}_{i=1}^{n_p}$.

A GP is fully specified by its mean and covariance (aka kernel) function. The mean is typically assumed to be zero in practice and we choose a squared-exponential kernel function, which is built on the assumption that feature variables close to each other (in terms of squared Euclidean distance) have similar robustnesses. The covariance between any two function values \mathbf{z}_i and $\mathbf{z}_{i'}$, $i, i' \in \{1, \dots, n_p\}$, is then given by [26, (6)]:

$$\mathbf{k}(\mathbf{z}_i, \mathbf{z}_{i'}) = \sigma_\rho^2 \exp\left(\frac{1}{2}(\mathbf{z}_i - \mathbf{z}_{i'})^T L_\rho^{-1}(\mathbf{z}_i - \mathbf{z}_{i'})\right) + \delta(\mathbf{z}_i, \mathbf{z}_{i'})\sigma_\delta^2, \quad (9)$$

where L_ρ is the diagonal length-scale matrix with positive values, $\delta(\cdot)$ is the Kronecker delta function, and σ_ρ and σ_δ are the process deviation and discretization noise, respectively. The parameters of the kernel function (9) can be obtained by maximizing the marginal log-likelihood using gradient-based optimization approaches [24, Sec. 5.1].

As a result, the training data \mathcal{D} and the output y^* at any particular input $\mathbf{z} = \mathbf{z}^*$ follow the joint distribution:

$$\begin{pmatrix} \mathbf{y} \\ y^* \end{pmatrix} \sim \mathcal{N}\left(\mathbf{0}_{n_p+1}, \begin{pmatrix} \mathbf{K} & \mathbf{k}^T(\mathbf{z}^*) \\ \mathbf{k}(\mathbf{z}^*) & \mathbf{k}(\mathbf{z}^*, \mathbf{z}^*) \end{pmatrix}\right), \quad (10)$$

where $\mathbf{y} = (y_1, \dots, y_{n_p})^T$ is the vector of observed outputs, $\mathbf{0}_{n_p+1} \in \mathbb{R}^{n_p+1}$ is a vector of zeros, $\mathbf{K} \in \mathbb{R}^{n_p \times n_p}$ is the covariance matrix with entries $K_{i,i'} = \mathbf{k}(\mathbf{z}_i, \mathbf{z}_{i'})$, and $\mathbf{k}(\mathbf{z}^*) = (\mathbf{k}(\mathbf{z}_1, \mathbf{z}^*), \dots, \mathbf{k}(\mathbf{z}_{n_p}, \mathbf{z}^*))$ contains the covariances evaluated at all training data and observation pairs. The prediction of the model is a conditional probability distribution of y^* given \mathcal{D} , which remains a Gaussian distribution with $P(y^*|\mathcal{D}) = \mathcal{N}(\mu(\mathbf{z}^*), \sigma^2(\mathbf{z}^*))$ [24, Sec. 2.2] and

$$\begin{aligned} \mu(\mathbf{z}^*) &= \mathbf{k}(\mathbf{z}^*)\mathbf{K}^{-1}\mathbf{y}, \\ \sigma^2(\mathbf{z}^*) &= \mathbf{k}(\mathbf{z}^*, \mathbf{z}^*) - \mathbf{k}(\mathbf{z}^*)\mathbf{K}^{-1}\mathbf{k}^T(\mathbf{z}^*). \end{aligned} \quad (11)$$

C. Robustness Prediction

To avoid false negatives and false positives, i.e., to ensure the soundness of the prediction (cf. Prop. 1), we rectify the mean value using the characteristic function (cf. Def. 1) to obtain the estimated model predictive robustness $\hat{\rho}^{\text{MP}}$ as:

$$\hat{\rho}^{\text{MP}}(p, \omega, k) = \begin{cases} \max(\mu(\omega(\omega_k)), 0) & \text{if } c(p, \omega, k) = 1 \\ \min(\mu(\omega(\omega_k)), 0) & \text{if } c(p, \omega, k) = -1 \end{cases}, \quad (12)$$

where the value of the predicted robustness with incorrect signs is set to 0. With the deviation $\sigma(\mathbf{z}^*)$, one can also obtain the confidence intervals on the computation. Since \mathbf{K} only needs to be inverted once for a given dataset, the complexities of evaluating the mean and variance in (11) are both $\mathcal{O}(n_d^2)$ [24, Alg. 2.1]. For applications with large amounts of data points, a sparse approximation of the GP regression [41] can be used to reduce the runtime complexity.

V. NUMERICAL EXPERIMENTS

We evaluate the applicability and efficacy of the model predictive robustness using the highD dataset [42] and German interstate traffic rules from [3], [8]. Our simulation is based on *CommonRoad* [43], and *GPpyTorch* [44] is used to model and solve the GP regression. We use the vehicle model from [45, (8) and (13)], which separates the longitudinal and lateral motion of the vehicle in the curvilinear coordinate system (cf. Fig. 2). The trajectories for all rule-relevant vehicles described in Sec. III are determined with a time horizon of $h\Delta t = 1.5s$ with step size $\Delta t = 0.04s$. The number of the sampled trajectories for the ego vehicle is set to 729. The GP regression model is trained with $n_p = 10,000$ data points when $|\mathcal{B}| > 0$, otherwise $n_p = 3,000$. The code used in this paper is published as open-source at <https://gitlab.lrz.de/tum-cps/mpr>.

A. Comparison with Related Work

Tab. II summarizes the fulfilling properties (cf. Sec. II-C) of the model-free and model predictive robustness. The monotonicity and soundness of the model predictive robustness hold by definition. The smoothness of the robustness is fulfilled using the GP regression and smooth approximations of the min and max operators in (11)³.

In addition, we consider comprehensive feature variables as inputs for the robustness prediction and can assess their predictive relevance utilizing the GP models. In contrast, the use of handcrafted functions might lead to the lack of considered variables for complex predicates, which we demonstrate in the following example:

Example: Consider the predicate `in_same_lane(x_{ego}, x_b)` [3] which describes whether the ego vehicle shares a lane with the vehicle $b \in \mathcal{B}$:

$$\text{in_same_lane}(x_{\text{ego}}, x_b) := |\mathcal{L}_{\text{ego}} \cap \mathcal{L}_b| > 0. \quad (13)$$

The calculation of its model-free robustness in [8, (1)] is sophisticated but only considers the positional attributes as the signed distance to the lanes occupied by the other vehicle, which is hardly normalizable and generalizable. For our approach, we use the variance of the GP posterior latent mean [46] to analyze the sensitivity of the feature variables. The distribution in Fig. 6 shows that not only the relative distance to the lane bounds but also the relative velocity has a comparably large feature relevance. This aligns with the human intuition of the factors affecting the robustness of

TABLE II: Comparison of properties with related work. Note that we examine the satisfaction of properties for all predicates.

Property	Model-free [8]	Model Predictive
Soundness	✓	✓
Smoothness	✗	✓
Monotonicity	✗	✓

³The mean $\mu(\mathbf{z}^*)$ is a linear combination of the squared-exponential kernel functions contained in $\mathbf{k}(\mathbf{z}^*)$ (cf. (11)), which are infinitely differentiable with respect to \mathbf{z}^* [24, Sec. 4.2.1]. The smooth approximations of the min and max operator in (12) can be found in [14] and [16].

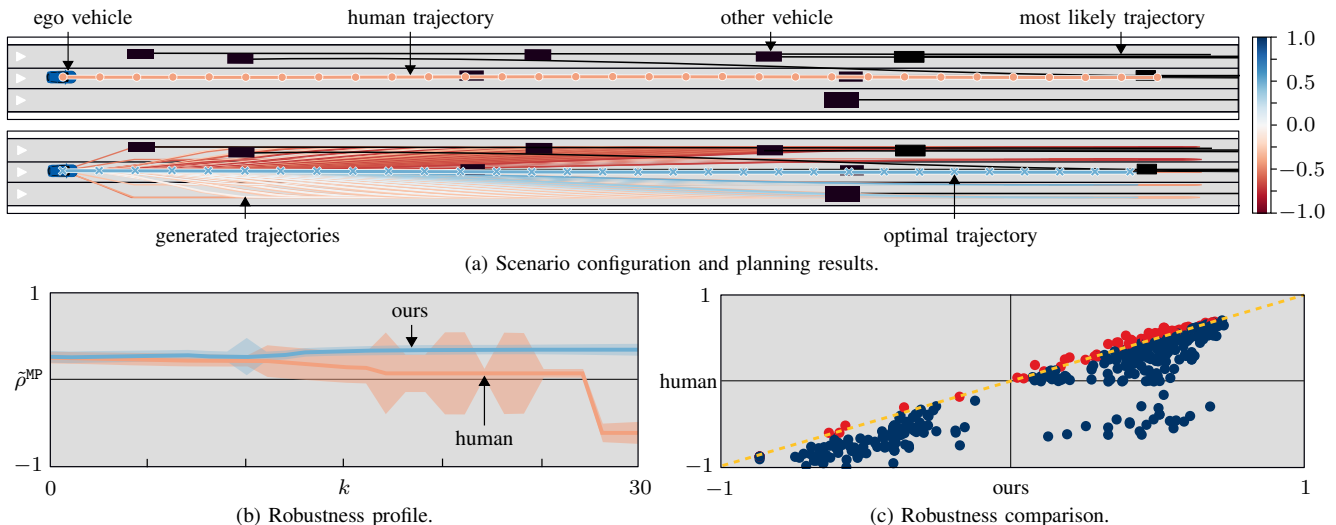


Fig. 5: Model-predictive-robustness-aware trajectory planning. The trajectories in (a) are color-coded according to the robustness, which increases from red with negative to blue with positive values. The shaded regions in (b) denote the $2\text{-}\sigma$ model uncertainty corresponding to a 95.4% confidence level. The right region of the dashed line in (c) is where the robustness of the optimal trajectory is greater than the one of the human trajectory.

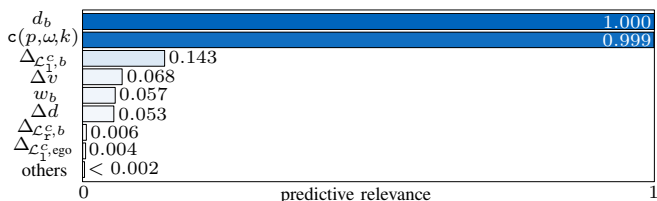


Fig. 6: Sensitivity analysis of the feature variables when evaluating the model predictive robustness of the predicate `in_same_lane`. The values are scaled so that the most relevant feature variable has a relevance of one.

two vehicles to stay in the same lane, e.g., the variables for calculating the time-to-line-crossing [47, Tab. I].

B. Robustness-aware Trajectory Planning

Our robustness measure can be easily integrated into the prediction of traffic rule violations [8] and trajectory repairing [13]. In this section, we demonstrate that the model-predictive definition also facilitates the robustness awareness of trajectory planning using a sampling-based planner of [36]. The model predictive robustness of rules R_G1 to R_G3⁴ from [3] is integrated as an additional robustness term J_r with weight $\lambda_r \in \mathbb{R}^+$ in the cost function J to the planner:

$$J(x, u) = J_p(x, u) - \lambda_r J_r(x, u), \quad (14)$$

where the performance term J_p is obtained from [36], (4) and the robustness calculation of STL operators is based on [6, Def. 3]. During planning, the collision-free sample with the minimum cost is selected as the optimal trajectory.

We show an exemplary scenario in Fig. 5a, where 450 trajectories are generated with a time increment of $0.2s$ and a horizon of 30 time steps. The robustness distribution of the selected optimal trajectory is compared to the one of the recorded human trajectory in Fig. 5b. The human driver does not keep a safe distance to the preceding vehicle for $k \in [28, 30]$, i.e., the rule R_G1 is violated. Including

⁴R_G1: Safe distance to preceding vehicle; R_G2: Unnecessary braking; R_G3: Maximum speed limit.

robustness as part of the cost function, the ego vehicle executes a braking maneuver to obey traffic rules as much as possible but with the least effort.

Furthermore, we evaluate the model-predictive-robustness-aware planning algorithm on 500 highD scenarios. As illustrated in Fig. 5c, over 85% of the planned trajectories have higher robustness than the recorded ones. The results show that the model predictive robustness helps to enhance the degree of traffic rule compliance of autonomous vehicles, which significantly outperforms human drivers in the evaluated dataset.

VI. CONCLUSIONS

This paper examines how one can precisely and quickly quantify the level of satisfaction or violation of STL predicates considering the environment and dynamic models. Unlike existing model-free robustness definitions, our proposed model predictive robustness not only grows monotonically as the satisfaction probability increases but also is sound and smooth in the sense of Prop. 1-3. With this, our method can be useful in terms of rule-compliant planning and control for autonomous vehicles. Future work will focus on incorporating our definition into other STL variants and employing model predictive robustness in an optimization framework to synthesize controllers as well as repair rule-violating trajectories.

ACKNOWLEDGMENTS

The authors kindly thank Patrick Halder for his valuable suggestions on earlier drafts of this paper and Ethan Tatlow for the voice-over in the video attachment. The authors also gratefully acknowledge partial financial support by the German Federal Ministry for Digital and Transport (BMDV) within the project *Cooperative Autonomous Driving with Safety Guarantees* (KoSi).

REFERENCES

- [1] M. Luckcuck, M. Farrell, L. A. Dennis, C. Dixon, and M. Fisher, "Formal specification and verification of autonomous robotic systems: A survey," *ACM Computing Surveys*, vol. 52, no. 5, pp. 1–41, 2019.
- [2] K. Esterle, L. Gressenbuch, and A. Knoll, "Formalizing traffic rules for machine interpretability," in *Proc. of the IEEE Connected and Automated Veh. Symp.*, 2020, pp. 1–7.
- [3] S. Maierhofer, A.-K. Rettinger, E. C. Mayer, and M. Althoff, "Formalization of interstate traffic rules in temporal logic," in *Proc. of the IEEE Intell. Veh. Symp.*, 2020, pp. 752–759.
- [4] N. Aréchiga, "Specifying safety of autonomous vehicles in signal temporal logic," in *Proc. of the IEEE Intell. Veh. Symp.*, 2019, pp. 58–63.
- [5] G. E. Fainekos and G. J. Pappas, "Robustness of temporal logic specifications for continuous-time signals," *Theoretical Computer Science*, vol. 410, no. 42, pp. 4262–4291, 2009.
- [6] A. Donzé and O. Maler, "Robust satisfaction of temporal logic over real-valued signals," in *Proc. of the Int. Conf. on Formal Modeling and Analysis of Timed Systems*, 2010, pp. 92–106.
- [7] E. Bartocci, J. Deshmukh, A. Donzé, G. Fainekos, O. Maler, D. Ničković, and S. Sankaranarayanan, "Specification-based monitoring of cyber-physical systems: A survey on theory, tools and applications," in *Lectures on Runtime Verification*. Cham: Springer, 2018, pp. 135–175.
- [8] L. Gressenbuch and M. Althoff, "Predictive monitoring of traffic rules," in *Proc. of the IEEE Int. Conf. on Intell. Transp. Syst.*, 2021, pp. 915–922.
- [9] S. Maierhofer, P. Moosbrugger, and M. Althoff, "Formalization of intersection traffic rules in temporal logic," in *Proc. of the IEEE Intell. Veh. Symp.*, 2022, pp. 1135–1144.
- [10] H. Krasowski and M. Althoff, "Temporal logic formalization of marine traffic rules," in *Proc. of the IEEE Intell. Veh. Symp.*, 2021, pp. 186–192.
- [11] M. Hekmatnejad, S. Yaghoubi, A. Dokhanchi, H. B. Amor, A. Shrivastava, L. Karam, and G. Fainekos, "Encoding and monitoring responsibility sensitive safety rules for automated vehicles in signal temporal logic," in *Proc. of the ACM/IEEE Int. Conf. on Formal Methods and Models for System Design*, 2019, pp. 1–11.
- [12] W. Xiao, N. Mehdipour, A. Collin, A. Y. Bin-Nun, E. Frazzoli, R. D. Tebbens, and C. Belta, "Rule-based optimal control for autonomous driving," in *Proc. of the ACM/IEEE Int. Conf. on Cyber-Physical Systems*, 2021, pp. 143–154.
- [13] Y. Lin and M. Althoff, "Rule-compliant trajectory repairing using satisfiability modulo theories," in *Proc. of the IEEE Intell. Veh. Symp.*, 2022, pp. 449–456.
- [14] Y. V. Pant, H. Abbas, and R. Mangharam, "Smooth operator: Control using the smooth robustness of temporal logic," in *Proc. of the IEEE Conf. on Control Technology and Applications*, 2017, pp. 1235–1240.
- [15] N. Mehdipour, C.-I. Vasile, and C. Belta, "Arithmetic-geometric mean robustness for control from signal temporal logic specifications," in *Proc. of the IEEE American Control Conf.*, 2019, pp. 1690–1695.
- [16] Y. Gilpin, V. Kurtz, and H. Lin, "A smooth robustness measure of signal temporal logic for symbolic control," *IEEE Control Systems Letters*, vol. 5, no. 1, pp. 241–246, 2020.
- [17] P. Varnai and D. V. Dimarogonas, "On robustness metrics for learning STL tasks," in *Proc. of the IEEE American Control Conf.*, 2020, pp. 5394–5399.
- [18] V. Kurtz and H. Lin, "Mixed-integer programming for signal temporal logic with fewer binary variables," *IEEE Control Systems Letters*, vol. 6, pp. 2635–2640, 2022.
- [19] C. Yoo and C. Belta, "Control with probabilistic signal temporal logic," *arXiv preprint arXiv:1510.08474*, 2015.
- [20] D. Sadigh and A. Kapoor, "Safe control under uncertainty with probabilistic signal temporal logic," in *Proc. of Robotics: Science and Systems XII*, 2016.
- [21] M. Tiger and F. Heintz, "Incremental reasoning in probabilistic signal temporal logic," *Int. J. of Approximate Reasoning*, vol. 119, pp. 325–352, 2020.
- [22] K. M. B. Lee, C. Yoo, and R. Fitch, "Signal temporal logic synthesis as probabilistic inference," in *Proc. of the IEEE Int. Conf. on Robotics and Automation*, 2021, pp. 5483–5489.
- [23] T. Nyberg, C. Pek, L. Dal Col, C. Norén, and J. Tumova, "Risk-aware motion planning for autonomous vehicles with safety specifications," in *Proc. of the IEEE Intell. Veh. Symp.*, 2021, pp. 1016–1023.
- [24] C. E. Rasmussen and C. K. Williams, *Gaussian processes for machine learning*. Cambridge: MIT press, 2006.
- [25] J. Kocijan, R. Murray-Smith, C. E. Rasmussen, and A. Girard, "Gaussian process model based predictive control," in *Proc. of the IEEE American Control Conf.*, 2004, pp. 2214–2219.
- [26] F. Berkenkamp and A. P. Schoellig, "Safe and robust learning control with Gaussian processes," in *Proc. of the IEEE European Control Conf.*, 2015, pp. 2496–2501.
- [27] L. Hewing, J. Kabzan, and M. N. Zeilinger, "Cautious model predictive control using Gaussian process regression," *IEEE Trans. on Control Systems Technology*, vol. 28, no. 6, pp. 2736–2743, 2019.
- [28] T. R. Torben, J. A. Glomsrud, T. A. Pedersen, I. B. Utne, and A. J. Sørensen, "Automatic simulation-based testing of autonomous ships using Gaussian processes and temporal logic," *Proc. of the Institution of Mechanical Engineers, Part O: J. of Risk and Reliability*, 2022.
- [29] E. Héry, S. Masi, P. Xu, and P. Bonnifait, "Map-based curvilinear coordinates for autonomous vehicles," in *Proc. of the IEEE Int. Conf. on Intell. Transp. Systems*, 2017, pp. 1–7.
- [30] E. F. Camacho and C. B. Alba, *Model predictive control*. Springer science & business media, 2013.
- [31] D. Koller and N. Friedman, *Probabilistic graphical models: principles and techniques*. MIT press, 2009.
- [32] K. P. Murphy, *Dynamic bayesian networks: Representation, inference and learning*. University of California, Berkeley, 2002.
- [33] M. Althoff, O. Stursberg, and M. Buss, "Model-based probabilistic collision detection in autonomous driving," *IEEE Trans. on Intell. Transp. Systems*, vol. 10, no. 2, pp. 299–310, 2009.
- [34] J. Hammersley, *Monte carlo methods*. Springer Science & Business Media, 2013.
- [35] T. M. Howard, C. J. Green, A. Kelly, and D. Ferguson, "State space sampling of feasible motions for high-performance mobile robot navigation in complex environments," *J. of Field Robotics*, vol. 25, no. 6-7, pp. 325–345, 2008.
- [36] M. Werling, S. Kammel, J. Ziegler, and L. Gröll, "Optimal trajectories for time-critical street scenarios using discretized terminal manifolds," *The Int. J. of Robotics Research*, vol. 31, no. 3, pp. 346–359, 2012.
- [37] C. Pek, V. Rusinov, S. Manzinger, M. C. Üste, and M. Althoff, "CommonRoad Drivability Checker: Simplifying the development and validation of motion planning algorithms," in *Proc. of the IEEE Intell. Veh. Symp.*, 2020, pp. 1013–1020.
- [38] P. Karle, M. Geisslinger, J. Betz, and M. Lienkamp, "Scenario understanding and motion prediction for autonomous vehicles - review and comparison," *IEEE Trans. on Intell. Transp. Systems*, pp. 1–21, 2022.
- [39] T. Gindele, S. Brechtel, and R. Dillmann, "A probabilistic model for estimating driver behaviors and vehicle trajectories in traffic environments," in *Proc. of the IEEE Int. Conf. on Intell. Transp. Syst.*, 2010, pp. 1625–1631.
- [40] X. Wang, H. Krasowski, and M. Althoff, "Commonroad-RL: A configurable reinforcement learning environment for motion planning of autonomous vehicles," in *Proc. of the IEEE Int. Conf. on Intell. Transp. Syst.*, 2021, pp. 466–472.
- [41] J. Quinero-Candela and C. E. Rasmussen, "A unifying view of sparse approximate Gaussian process regression," *The J. of Machine Learning Research*, vol. 6, pp. 1939–1959, 2005.
- [42] R. Krajewski, J. Bock, L. Kloeker, and L. Eckstein, "The highD dataset: A drone dataset of naturalistic vehicle trajectories on German highways for validation of highly automated driving systems," in *Proc. of the IEEE Int. Conf. on Intell. Transp. Syst.*, 2018, pp. 2118–2125.
- [43] M. Althoff, M. Koschi, and S. Manzinger, "CommonRoad: Composable benchmarks for motion planning on roads," in *Proc. of the IEEE Intell. Veh. Symp.*, 2017, pp. 719–726.
- [44] J. Gardner, G. Pleiss, K. Q. Weinberger, D. Bindel, and A. G. Wilson, "GPYtorch: Blackbox matrix-matrix gaussian process inference with GPU acceleration," in *Proc. of the Conf. on Neural Information Processing Systems*, 2018, pp. 7576–7586.
- [45] C. Pek and M. Althoff, "Fail-safe motion planning for online verification of autonomous vehicles using convex optimization," *IEEE Trans. on Robotics*, vol. 37, no. 3, pp. 798–814, 2021.
- [46] T. Paananen, J. Piironen, M. R. Andersen, and A. Vehtari, "Variable selection for Gaussian processes via sensitivity analysis of the posterior predictive distribution," in *Proc. of the Int. Conf. on Artificial Intell. and Statistics*, 2019, pp. 1743–1752.
- [47] S. Mammars, S. Glaser, and M. Netto, "Time to line crossing for lane departure avoidance: A theoretical study and an experimental setting," *IEEE Trans. on Intell. Transp. systems*, vol. 7, no. 2, pp. 226–241, 2006.